

Report NW-02



**Direct Displacement Procedure for Performance-Based  
Seismic Design of Multistory Woodframe Structures**

By

**Weichiang Pang  
and  
David Rosowsky**

Zachry Department of Civil Engineering  
Texas A&M University  
College Station, Texas 44843-3136

June 2007

**Development of a Performance-Based Seismic Design  
Philosophy for Mid-Rise Woodframe Construction**

[www.engr.colostate.edu/NEESWood](http://www.engr.colostate.edu/NEESWood)

Project Sponsored by the



National Science Foundation  
WHERE DISCOVERIES BEGIN



NEES



Rensselaer

TEXAS A&M  
ENGINEERING

## **Disclaimer**

This material is based upon work supported by the National Science Foundation under Grant No. CMMI-0529903 (NEES Research) and CMMI-0402490 (NEES Operations). Any opinions, findings, and conclusions or recommendations expressed in this material are those of the investigators and do not necessarily reflect the views of the National Science Foundation.

## **PROJECT OVERVIEW**

### **NEESWood: Development of a Performance-Based Seismic Design Philosophy for Mid-Rise Woodframe Construction**

While woodframe structures have historically performed well with regard to life safety in regions of moderate to high seismicity, these types of low-rise structures have sustained significant structural and non-structural damage in recent earthquakes. To date, the height of woodframe construction has been limited to approximately four stories, mainly due to the lack of understanding of the dynamic response of taller (mid-rise) woodframe construction, non-structural limitations such as material fire requirements, and potential damage considerations for non-structural finishes. Current building code requirements for engineered wood construction around the world are not based on a global seismic design philosophy. Rather, wood elements are designed independently of each other without consideration of the influence that their stiffness and strength have on the other structural components of the structural system. Furthermore, load paths in woodframe construction arising during earthquake shaking are not well understood. These factors, rather than economic considerations, have limited the use of wood to low-rise construction and, thereby, have reduced the economical competitiveness of the wood industry in the U.S. and abroad relative to the steel and concrete industry. This project seeks to take on the challenge of developing a seismic design philosophy that will provide the necessary mechanisms to safely increase the height of woodframe structures in active seismic zones of the U.S. as well as mitigating damage to low-rise woodframe structures. This will be accomplished through the development of a new seismic design philosophy that will make mid-rise woodframe construction a reality in regions of moderate to high seismicity. Such a design philosophy falls under the umbrella of the performance-based design paradigm.

In Year 1 of the NEESWood Project, a full-scale seismic benchmark tests of a two-story woodframe townhouse unit that required the simultaneous use of the two three-dimensional shake tables at the SUNY- Buffalo NEES node will be performed. As the largest full-scale three-dimensional shake table test ever performed in the U.S., the results of this series of shake table tests on the townhouse will serve as a benchmark for both woodframe performance and nonlinear models for seismic analysis of woodframe structures. These efficient analysis tools will provide a platform upon which to build the performance-based seismic design (PBSD) philosophy. The PBSD methodology will rely on the development of key performance requirements such as limiting inter-story deformations. The method will incorporate the use of economical seismic protection systems such as supplemental dampers and base isolation systems in order to further increase energy dissipation capacity and/or increase the natural period of the woodframe buildings.

The societal impacts of this new PBSD procedure, aimed at increasing the height of woodframe structures equipped with economical seismic protection systems, will also be investigated within the scope of this NEESWood project. Once the PBSD philosophy for mid-rise (and all) woodframe structures has been developed, it will be applied to the seismic design of a mid-rise (six-story) multi-family residential woodframe condominium/apartment building. This mid-rise woodframe structure will be constructed and tested at full-scale in a series of shake table tests on the E-Defense (Miki) shake table in Japan. The use of the E-Defense shake table, the largest 3-D shake table in the world, is necessary to accommodate the height and payload of the mid-rise building. There will be a general solicitation in the U.S. and in the international earthquake engineering community for payload projects to be conducted during this series of tests, thus maximizing the benefit to cost ratio for the world's earthquake engineering community. This additional objective of developing collaborative linkages between NEES and Japan's National Institute for Earth Science and Disaster Prevention (NIED) E-Defense Project will help form the "...global seamless network for earthquake engineering...".

The **intellectual merit** of NEESWood is the development of a new design philosophy that will provide a logical, economical basis for the design of mid-rise woodframe construction. Numerous contributions to earthquake engineering will result from successful completion of the NEESWood Project.

The **broader impacts** of NEESWood are that it will provide a seminal advancement in seismic design of woodframe construction. When this challenge is successfully met, mid-rise woodframe construction will be an economic option in seismic regions around the U.S. and the world.

## Project Team

<b>John W. van de Lindt</b> , Ph.D., Principal Investigator: Associate Professor, Department of Civil Engineering, Colorado State University, Fort Collins, CO 80523-1372; <a href="mailto:jwv@engr.colostate.edu">jwv@engr.colostate.edu</a>
<b>Rachel A. Davidson</b> , Ph.D., Co-Principal Investigator: Associate Professor, Department of Civil and Environmental Engineering, University of Delaware, Newark, DE 19716-3120
<b>Andre Filiatrault</b> , Ph.D. Eng., Co-Principal Investigator: Deputy Director of the Multidisciplinary Center for Earthquake Engineering Research (MCEER) and Professor Department of Civil, Structural, and Environmental Engineering, State University of New York at Buffalo, Red Jacket Quadrangle, Buffalo, New York 14261; <a href="mailto:af36@buffalo.edu">af36@buffalo.edu</a> .
<b>David V. Rosowsky</b> , Ph.D., Co-Principal Investigator: A.P. Florence Wiley Chair Professor and Department Head, Texas A&M University, Zachry Department of Civil Engineering, College Station, TX 77843-3136; <a href="mailto:rosowsky@tamu.edu">rosowsky@tamu.edu</a> .
<b>Michael D. Symans</b> , Ph.D., Co-Principal Investigator: Associate Professor, Department of Civil and Environmental Engineering, Rensselaer Polytechnic Institute, 110 8 <sup>th</sup> Street, Troy, NY 12180-3590; <a href="mailto:symans@rpi.edu">symans@rpi.edu</a> .

## **Acknowledgements**

The authors would like to thank Mr. Ioannis Christovasilis and Professor Andre Filiatrault of the State University of New York at Buffalo, and Professor John van de Lindt of Colorado State University for their critical review and constructive comments on an earlier draft of this report.

# Table of Contents

Disclaimer .....	ii
Project Overview .....	iii
Acknowledgements .....	v
Table of Contents .....	vi
List of Figures .....	vii
List of Tables .....	viii
Abstract .....	ix
1. Introduction .....	1
2. Current Force-based Design Procedure.....	1
3. Direct Displacement Design for Multistory Woodframe Structures.....	4
3.1 Design Performance Levels .....	6
3.2 Design Acceleration Response Spectrum .....	7
3.2.1 Adjustment for Hazard Level or Return Period.....	7
3.2.2 Adjustment for Site Class .....	9
3.3 Shearwall Backbone Curve.....	11
3.4 Equivalent Linearization of Nonlinear Backbone Curve.....	12
3.5 Shearwall Backbone Design Table .....	14
3.6 Normalized Modal Analysis .....	16
3.7 Design Inter-story Drift Spectra.....	18
3.8 Required Equivalent First-floor Period and Stiffness.....	20
3.9 Required Base Shear, Story Shear and Uplift Force.....	20
4. Design Example .....	21
4.1 Description of Three-Story Woodframe Structure .....	21
4.2 Design Process .....	22
4.3 Verification of DDD using Nonlinear MDOF Dynamic Analyses.....	27
5. Conclusions .....	30
References.....	32

## List of Figures

Figure 1:	(a) Design acceleration response spectrum, (b) Design base shear obtained via force reduction factor, $R$ (force-based design).....	2
Figure 2:	Flowchart for multi-story DDD procedure. ....	5
Figure 3:	5%-damped design acceleration response spectra for LA City Hall, Los Angeles, California. ....	10
Figure 4:	Shearwall backbone curve parameters.....	12
Figure 5:	Equivalent linearization of nonlinear backbone curve. ....	13
Figure 6:	Summation of shearwall segment backbone curves. ....	15
Figure 7:	Equivalent linearization of a nonlinear MDOF system. ....	16
Figure 8:	Construction of an inter-story drift spectrum. ....	19
Figure 9:	Determination of the required first-floor period. ....	19
Figure 10:	Elevation views of three-story woodframe structure.....	22
Figure 11:	Direct displacement design for the CP performance level. ....	23
Figure 12:	Response spectra for the 10%/50yr bi-axial ground motions. ....	27
Figure 13:	Three-dimensional nonlinear model for a three-story woodframe structure. ....	28
Figure 14:	Peak drift distributions from nonlinear dynamic analyses (CP hazard level). ....	29

## List of Tables

Table 1:	Design performance levels of woodframe shearwalls per FEMA 356. ....	6
Table 2:	Values of exponents use to determine response acceleration parameters. .	8
Table 3:	Site Class adjustment parameters. ....	9
Table 4:	Damping coefficients. ....	10
Table 5:	Acceleration response spectra parameters. ....	10
Table 6:	Displacement-based shearwall design table for walls built with studs spaced at 400 mm (16 in) on-center and OSB attached using 8d common nails. ....	15
Table 7:	Displacement-based design of east and west walls for multiple performance levels. ....	25
Table 8:	X-direction design story shears for multiple performance levels. ....	26
Table 9:	Determination of X-direction peak backbone forces and design story shears for the CP performance level. ....	26
Table 10:	Average peak drift responses from nonlinear dynamic analyses for different hazard levels. ....	30

## Abstract

While performance-based seismic design (PBSD) concepts have evolved for steel and concrete structures over the last decade, PBSD concepts have only recently been explored for engineered wood structures. An important development in PBSD has been the introduction of direct displacement design (DDD) procedures. This paper presents a displacement-based design procedure that can be used for PBSD of multistory woodframe structures. The procedure does not require nonlinear dynamic time-history analysis of the complete structure. Instead, only simple modal analysis and knowledge of the backbone response of the participating shearwall segments are needed. In the design process, the acceleration response spectrum is converted into a set of inter-story drift spectra which is used to determine the minimum stiffness required for each floor in order to maintain the drift level below certain design limits. The structure is assumed to have symmetric plan and rigid diaphragms, assumptions that greatly simplify the analysis (i.e., no torsional effects), and yet are reasonable for most wood structures of regular plan. As an illustrative example, the design of a three-story woodframe structure is presented. The validity of the proposed DDD procedure is confirmed using results from nonlinear dynamic time-history analyses of the complete structure. The target DDD inter-story drift profiles closely matched the average peak inter-story drifts obtained from the time-history analyses.

## 1. Introduction

More than 90% of all structures built in the United States are woodframe. Current design procedures (including seismic) for woodframe construction are largely prescriptive in nature with one target objective, i.e., to ensure life safety. Recent earthquakes (e.g., Loma Prieta in 1989 and Northridge in 1994) have revealed that even when casualties were limited, the property losses and social disruption can be enormous and have the potential to become unmanageable. For example, in the 1994 Northridge earthquake, 19 of the total 57 fatalities were related to collapse or failure of woodframe structures and more than half of the approximately \$20B in property losses was the result of damage to wood structures (Homes and Somers, 1996). Immediately after the earthquake, more than 100,000 individuals were displaced from their homes because the structures were severely damaged and immediate re-occupancy was not possible. Considering the intensity and magnitude of these earthquakes, wood structures proved to be relatively effective with regard to *collapse prevention* and *life safety* but much less effective in limiting economic losses or ensuring *immediate occupancy* was possible following the event. These events demonstrate the need for performance-based seismic design (PBSD) procedures that will simultaneously meet both safety and damage limitation requirements.

The vast majority of woodframe structures, even those built in high hazard regions, are engineered to meet strength requirements using deemed-to-comply or other pre-engineered approaches. The implementation of a PBSD philosophy will require engineers to perform more advanced analysis of complete structures, often comprising a large number of complex and interconnected assemblies. Advances are being made in the area of “whole structure” modeling of wood structures, however it is likely that the majority of these structures will be designed by engineers without access to such modeling capabilities. Still, techniques will be needed to allow the engineers to evaluate expected structural performance under seismic loading and to compare this to target performance requirements (drift limits) without having to resort to fully dynamic modeling and analysis of the structure. This paper presents a multiple-objective direct displacement-based design (DDD) procedure for multistory woodframe structures. The proposed method can provide estimates of inter-story drift in multistory structures and yet can be performed without the need for nonlinear pushover analysis or dynamic time-history analysis of the complete structure.

## 2. Current Force-based Design Procedure

In the United States, seismic design of woodframe structures has traditionally followed force-based procedures. The basic steps in a force-based procedure, based on the current edition of International Building Code (ICC 2006) and the seismic design provisions included in the ASCE/SEI 7-05, Minimum Design Loads for Buildings and Other Structures, (ASCE 2005), are as follows:

1. **Period Determination** – The force-based procedure begins with an approximation of the elastic fundamental period of the structure,  $T_a$ , in the direction under consideration using an empirical equation provided by the design code:

$$T_a = C_t h_n^x \quad (1)$$

where  $h_n$  (m or ft) is the height of the structure and  $C_t$  is the approximate period parameter. For woodframe structures, the exponent  $x$  is equal to 0.75 and  $C_t$  is equal to 0.0488 or 0.02 when the structure height is expressed in SI or US customary units, respectively.

2. **Elastic Base Shear** – Next, the elastic spectral acceleration,  $S_a$ , based on the elastic fundamental period (Figure 1a) is used to calculate the required elastic base shear,  $V_E$ , as:

$$V_E = S_a I_E W \quad (2)$$

where  $W$  is the seismic weight and  $I_E$  is the occupancy important factor (a function of the use of the structure).

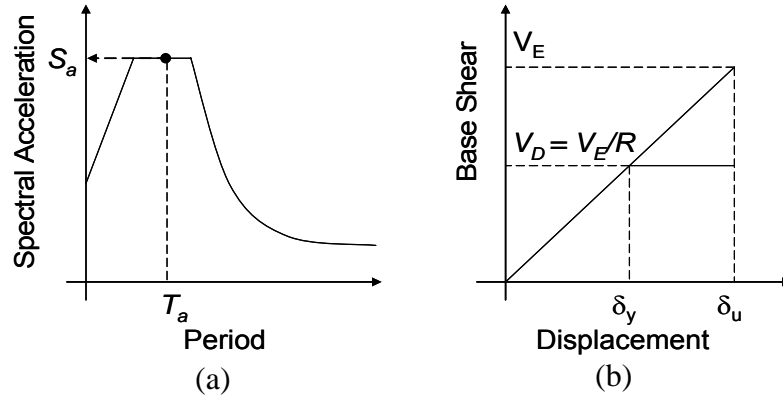


**Figure 1:** (a) Design acceleration response spectrum, (b) Design base shear obtained via force reduction factor,  $R$  (force-based design)

3. **Design Base Shear** – The design base shear,  $V_D$ , is then determined by dividing the elastic base shear by a response modification coefficient, commonly known as the force reduction factor,  $R$ , which accounts for the inelastic behavior of the structure (Figure 1b):

$$V_D = \frac{V_E}{R} \quad (3)$$

4. **Distribution of Story Forces** – Once the base-shear is determined, the design story shear for each floor is computed using a vertical distribution factor which is expressed in terms of story seismic weight and story height.
5. **Wood Shearwall Deflection** – The last step of the design procedure is to calculate the deflection of the shearwall using a four-term deflection equation given by the design code. The design code shearwall deflection equation includes terms to account for bending of the framing members, shear deformation of the sheathing panels, fastener slip, and hold-down slip. The design is revised if the displacement exceeds the allowable story drift.

Although easy to apply, many of the assumptions made in the force-based design are not applicable to woodframe structures. For example, and as discussed by Filiatrault and Folz (2002):

1. The approximate elastic fundamental period equation provided by the design code was not developed for woodframe structures. For example, the recorded initial fundamental periods for the two recently tested 5.48 m (18 ft) tall two-story woodframe structures (Filiatrault et al., 2007, Fischer et al., 2001) were around 0.3 seconds, while the design code specified empirical equation estimates the period at 0.17 seconds. Furthermore, the use of a single elastic period to design mid-rise woodframe structures is inappropriate since the force-displacement response of these wood buildings is highly nonlinear.
2. The use of an  $R$  factor to reduce the elastic base shear implies that, for a given seismic hazard, the maximum displacements for both the elastic and inelastic systems are the same (Figure 1b). This equal displacement assumption is not technically justified. Furthermore, the global load-displacement response of woodframe structures can not be adequately modeled using either linear-elastic or elastic-plastic models.
3. The  $R$  factor can be viewed as the global ductility factor of the structure. Both the yield and ultimate displacements must be identified in order to establish an  $R$  factor. This presents a major difficulty for establishing  $R$  factors for wood lateral load resisting systems since the yield point for woodframe structures can not be clearly defined.
4. The force-based procedure is a single-objective design procedure which focuses on reaching a target safety level for rare and severe earthquake events. However, ensuring structural damage is kept to a manageable level under earthquakes of moderate intensity is not explicitly considered. The deficiency of single-objective design was further made evident by the extensive damage to wood structures observed in recent earthquakes (e.g., Northridge 1994).
5. Force-based design is first performed at the global level to obtain the required base shear. The base shear is then distributed to each floor based on the story

weight and height. The story drift and stiffness are not directly addressed in the force-based procedure. As a result, the local drift response (inter-story drift) can not be properly assessed.

The shortcomings of using force-based design for wood structures have been identified by others (Filiatrault and Folz, 2002) and were discussed in a recent Workshop on performance-based design of woodframe structures (van de Lindt, 2005). Traditional force-based design procedures that considered only seismic force are unable to ensure multiple performance objectives are met, including damage and loss limitation. A recent experimental study has shown a strong correlation between displacement / drift and the level of damage observed during shake table tests of a wood structure (van de Lindt and Liu, 2006). Therefore, a design procedure that focuses on limiting inter-story drift might be a more rationale approach for PBSO of engineered woodframe buildings when damage limitation is one of the design objectives.

### **3. Direct Displacement Design for Multistory Woodframe Structures**

Displacement-based design was first suggested by Priestley (1998) as an alternative to full nonlinear time-history analysis of concrete structures. Filiatrault and Folz (2002) later adapted this approach and presented one possible displacement-based design procedure for wood structures. This design procedure was applied to a two-story woodframe building (Filiatrault et. al., 2006). The global behavior of the wood structure is modeled as an equivalent single-degree-of-freedom (SDOF) system with equivalent secant stiffness and equivalent viscous damping ratio. This design methodology addresses most of the deficiencies of the force-based procedure. However, the proposed method requires nonlinear pushover analysis of the complete structure, as well as an estimate of equivalent viscous damping at a target drift limit. As pointed out by the authors, these can be considered as disadvantages to a generalized procedure since nonlinear pushover analysis often requires the use of complex finite element programs. Furthermore, equivalent viscous damping ratios of wood structures have been quantified for only selected one to three-story structures (e.g., Camelo et. al., 2001; Filiatrault et. al., 2004) and damping values are not well established for taller woodframe structures.

Building on the foundation of the SDOF displacement-based design methodology, a design procedure for multiple-degree-of-freedom (MDOF) systems which requires neither nonlinear pushover analysis nor the equivalent viscous damping ratio was developed. The proposed DDD procedure is tailored specifically for multistory woodframe structures with the purpose of addressing the drawbacks of current force-based procedures. As previously mentioned, damage in wood structures can be directly related to displacement demand. In multistory DDD, inter-story drift is considered explicitly as a seismic design parameter at the beginning of the design process. The general steps for the multistory DDD procedure (shown in Figure 2) are as follows :

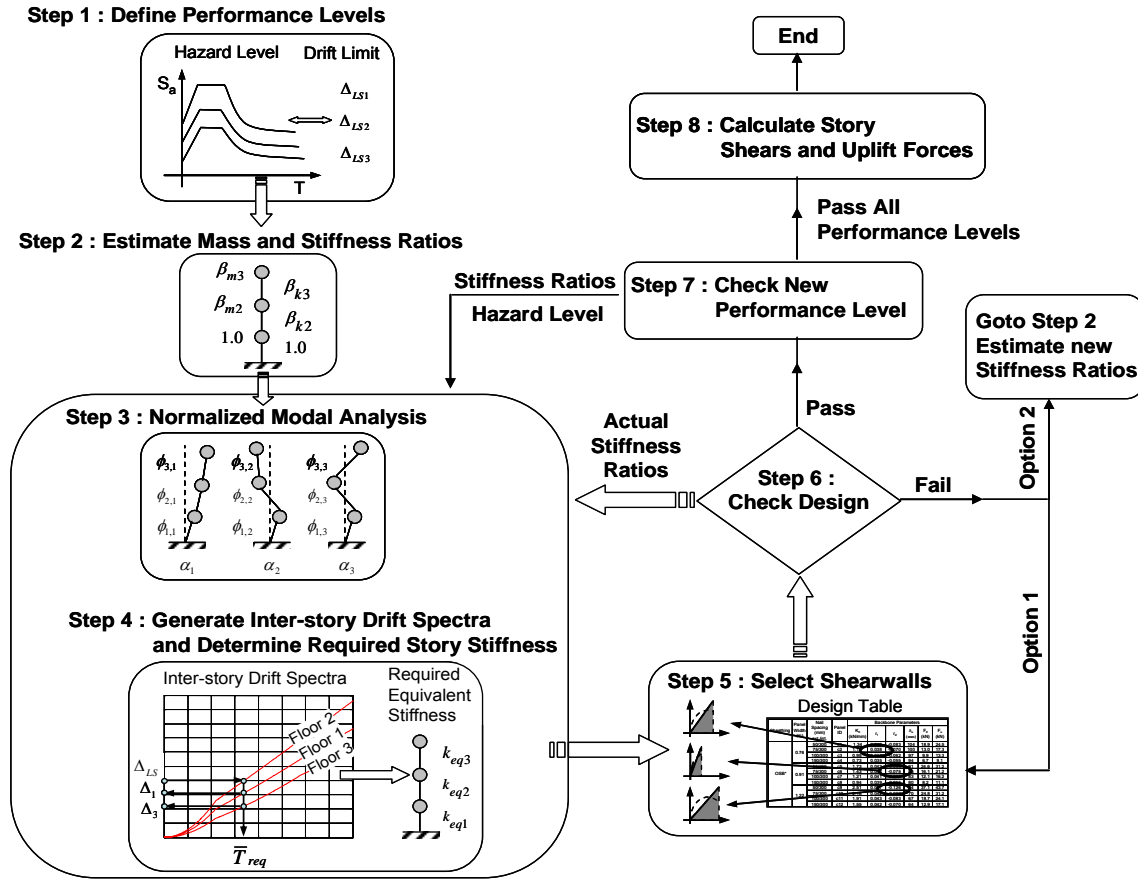


**Figure 2:** Flowchart for multi-story DDD procedure.

1. Define multiple performance levels in terms of limiting inter-story drifts for given seismic hazard levels.
2. Calculate or estimate the mass and stiffness ratios (relative to first floor) for each floor.
3. Perform normalized modal analysis on the equivalent linear MDOF system to obtain inter-story drift factors and natural frequency parameters.
4. Construct inter-story drift spectra for the most severe hazard level and determine the required equivalent stiffness for each floor.
5. Select lateral force resisting system from wood shearwall design tables which include information on shearwall backbone response and equivalent stiffnesses at various drift levels.
6. Check the design using the actual stiffness ratios (based on the shearwalls selected in step 5). Revise the shearwall selection if necessary.

7. Repeat steps 2 - 6 for each performance level using the actual stiffness ratios of the selected shearwalls. Revise the design if drift limits are exceeded at any performance levels.
8. Compute design base shear, story shear and uplift force using the actual nonlinear backbone curves of shearwalls.

The displacement-based procedure outlined above involves some new modeling techniques. The following sections will describe the procedure for linearization of nonlinear systems, the method to perform normalized modal analysis, the technique to generate inter-story drift spectra, and the development of displacement-based shearwall design tables.

### 3.1 Design Performance Levels

Recent major earthquakes demonstrated that woodframe structures built per prescriptive force-based design codes were relatively effective in preventing structural collapse but much less effective in ensuring economic losses are kept to manageable levels. In order to overcome this limitation, performance-based engineering concepts have evolved and are gaining acceptance among design engineers in North America and elsewhere. Performance-based seismic design procedures are formulated such that the resulting design will simultaneously meet multiple objectives or performance levels. In the case of seismic design, seismic hazard levels are coupled with target drift limits to form these performance levels.

Three performance levels, immediate occupancy (IO), life safety (LS), and collapse prevention (CP), defined in FEMA 356 (2000), are adopted herein to illustrate the proposed DDD procedure. Table 1 shows the FEMA 356 IO, LS, and CP performance requirements for wood shearwalls. While these three levels are used to illustrate the procedure herein, there is no limit to the number of hazard level / drift limit pairs that can be considered. Performance-based engineering not only means that structures can be designed to meet multiple objectives, it also implies that structures can be designed to meet owners' specifications or needs. The IO, LS, and CP performance levels can be viewed as the code specified minimum requirements. Informed building owners and/or engineers may specify additional performance levels to maximize the return of their investment or to provide protection to occupants beyond the code requirement (Krawinkler, 1999).

**Table 1:** Design performance levels of woodframe shearwalls per FEMA 356.

<b>Limit State</b>	<b>Seismic Hazard</b>	<b>Drift Limits</b>
Immediate Occupancy	50%/50yr	1%
Life Safety	10%/50yr	2%
Collapse Prevention	2%/50yr	3%

The objective of the IO performance level is to minimize significant economic loss when subjected to a moderate earthquake event having a 50% probability of exceedance in 50 years (50%/50yr). Damage to the woodframe structure or the resisting shearwalls is expected to be minor if the transient drift is kept below 1% of the story height. In general, structural repair is not required prior to re-occupancy.

For a more severe seismic event (10% probability of exceedance in 50 years, or 10%/50yr), the objective changes from loss prevention / minimization to reduction of risk of life-threatening injury to the occupants (i.e., life safety). It is assumed that with a maximum of 2% transient drift permitted, significant damage to the structure has occurred and the stiffness and strength have degraded but still provide a margin of safety against partial or total collapse.

At the CP performance level, the sole objective is to prevent loss of human life resulting from partial or total collapse of the structure. The CP performance level is coupled with rare and severe earthquake events having a return period of 2,475 years (2% probability of exceedance in 50 years, or 2%/50yr). Wood structures that meet the CP performance level are expected to remain standing with a maximum of 3% inter-story drift. However, non-life-threatening injury to the occupants and complete economic losses are acceptable at this level (FEMA 356, 2000).

## **3.2 Design Acceleration Response Spectrum**

The United States Geological Survey (USGS) had developed a set of national earthquake hazard maps. These probabilistic hazard maps can be used to generate horizontal acceleration design spectra using the procedure described in Section 1.6.1.5 of FEMA 356 (2000) for different seismic hazard levels.

Consider a site located near City Hall in Los Angeles, California (Lat. 34.05°, Long. -118.242°). The short-period,  $S_{S\_BSE1}$ , and one-second period,  $S_{I\_BSE1}$ , spectral acceleration parameters determined from the 2002 USGS hazard maps for Basic Safety Earthquake 1 (BSE-1) are 1.18 g and 0.40 g, respectively. The BSE-1 events correspond to earthquakes having a 10% probability of exceedance in 50 years. Similarly, for Basic Safety Earthquake 2 (BSE-2), the short-period,  $S_{S\_BSE2}$ , and one-second period,  $S_{I\_BSE2}$ , spectral acceleration parameters are 2.17 g and 0.73 g, respectively. In most areas of United States, BSE-2 events have a 2% probability of exceedance in 50 years. Using the FEMA 356 procedure, the mapped response acceleration parameters must then be adjusted for return periods or hazard levels (if the desired hazard level does not correspond to either 2%/50yr or 10% 50yr) and Site Class (soil type), accordingly. These adjustments are described below.

### **3.2.1 Adjustment for Hazard Level or Return Period**

For hazard levels between 2%/50yr and 10% 50yr, and  $S_{S\_BSE2}$  smaller than 1.5g, the short-period and one-second period response acceleration parameters adjusted for hazard level are given by Eqns (4) and (5) :

$$S_S = e^{\log(S_{S\_BSE1}) + [\log(S_{S\_BSE2}) - \log(S_{S\_BSE1})] \times [0.606 \log(PR) - 3.73]} \quad \text{for } S_{S\_BSE2} < 1.5g \quad (4)$$

$$S_I = e^{\log(S_{I\_BSE1}) + [\log(S_{I\_BSE2}) - \log(S_{I\_BSE1})] \times [0.606 \log(PR) - 3.73]} \quad \text{for } S_{S\_BSE2} < 1.5g \quad (5)$$

For all other hazard levels and  $S_{S\_BSE2}$  values, Eqns (6) and (7) are used:

$$S_S = S_{S\_BSE1} \left( \frac{P_R}{475} \right)^{n_S} \quad (6)$$

$$S_I = S_{I\_BSE1} \left( \frac{P_R}{475} \right)^{n_I} \quad (7)$$

where  $P_R$  is the mean return period (years) at the target exceedance probability in  $Y$  years,  $P_{EY}$ , calculated as:

$$P_R = \frac{-Y}{\ln(1 - P_{EY})} \quad (8)$$

Exponents  $n_S$  and  $n_I$  for different regions are listed in Table 2.

**Table 2:** Values of exponents use to determine response acceleration parameters.

Hazard Level	$\leq 10\%/50\text{yr}$ $\geq 2\%/50\text{yr}$		$> 10\%/50\text{yr}$		$> 10\%/50\text{yr}$	
	$\geq 1.5g$		$< 1.5g$		$\geq 1.5g$	
$S_{S\_BSE2}$ Region	$n_S$	$n_I$	$n_S$	$n_I$	$n_S$	$n_I$
California	0.29	0.29	0.44	0.44	0.44	0.44
Pacific Northwest	0.56	0.67	0.54	0.59	0.89	0.96
Intermountain	0.50	0.60	0.54	0.59	0.54	0.59
Central US	0.98	1.09	0.77	0.80	0.89	0.89
Eastern US	0.93	1.05	0.77	0.80	1.25	1.25

### 3.2.2 Adjustment for Site Class

Once the response acceleration parameters,  $S_S$  and  $S_I$ , are modified for return period, adjustment for Site Class or soil type is made using Eqns (9) and (10).

$$S_{XS} = F_a S_S \quad (9)$$

$$S_{X1} = F_v S_I \quad (10)$$

where  $S_{XS}$  and  $S_{X1}$  are the design short-period and one-second period spectral response acceleration parameters (g) modified for Site Class effect and  $F_a$  and  $F_v$  are site coefficients. For the location considered in this study, Site Class D (stiff soil) is assumed and the site coefficients are given in Table 3.

**Table 3:** Site Class adjustment parameters.

$S_S$ (g)	$\leq 0.25$	0.50	0.75	1.00	$\geq 1.25$
$F_a$	1.6	1.4	1.2	1.1	1.0
$S_I$ (g)	$\leq 0.10$	0.20	0.30	0.40	$\geq 0.50$
$F_v$	2.4	2.0	1.8	1.6	1.5

The design acceleration response spectrum is given by:

$$S_a(T) = \begin{cases} S_{XS} \left[ \left( \frac{5}{B_S} - 2 \right) \frac{T}{T_S} + 0.4 \right] & T < T_0 \\ \frac{S_{XS}}{B_S} & T_0 \leq T \leq T_S \\ \frac{S_{X1}}{B_1 T} & T > T_S \end{cases} \quad (11)$$

where  $T$  is the period (sec), and  $B_S$  and  $B_I$  are damping coefficients at short-period and one-second period, respectively. Periods  $T_S$  and  $T_0$  define the upper and lower limits of the plateau region of the design acceleration response spectrum and are given by,

$$T_S = \frac{S_{X1} B_S}{S_{XS} B_1} \quad (12)$$

$$T_0 = 0.2 T_S \quad (13)$$

The damping coefficients ( $B_S$  and  $B_I$ ) are functions of the effective viscous damping ratio,  $\beta$  (% of critical damping), and values for these coefficients are listed in Table 4. A viscous damping ratio of 5% can be assumed for most wood structures when determining

the design acceleration response spectrum. Other values for  $\beta$  are permitted if the conditions given in Section 1.6.1.5.3 of FEMA 356 (2000) are met.

**Table 4:** Damping coefficients.

Effective Viscous Damping (% of critical damping)	$\leq 2$	5	10	20	30	40	$\geq 50$
$B_s$	0.8	1.0	1.3	1.8	2.3	2.7	3.0
$B_I$	0.8	1.0	1.2	1.5	1.7	1.9	2.0

Figure 3 shows the design acceleration response spectra corresponding to IO, LS and CP performance levels for the selected site in Los Angeles, California, assuming Site Class D and an effective viscous damping ratio of 5% ( $B_s$  and  $B_I$  equal to 1). The parameters used to generate the design acceleration response spectra are given in Table 5. These acceleration design response spectra represent the seismic demand requirements for different performance levels.

**Table 5:** Acceleration response spectra parameters.

Seismic Hazard	$S_{xs}$ (g)	$S_{x1}$ (g)	$T_s$ (S)	$T_0$ (S)
50%/50yr	0.71	0.37	0.52	0.10
10%/50yr	1.21	0.65	0.53	0.11
2%/50yr	1.91	0.98	0.51	0.10

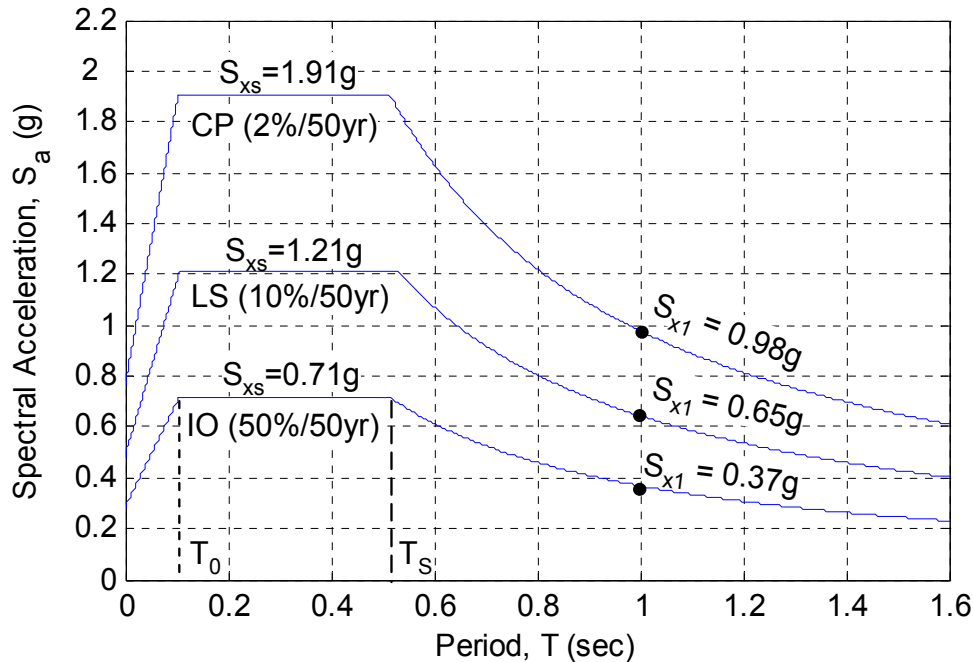


**Figure 3:** 5%-damped design acceleration response spectra for LA City Hall, Los Angeles, California.

### 3.3 Shearwall Backbone Curve

Shearwalls are essential elements of the primary lateral force resisting system in woodframe structures. Extensive monotonic pushover and cyclic tests of engineered woodframe shearwalls have shown that the top of the wall load versus displacement response is highly nonlinear (e.g., SEAOSC-UCI, 2001; Gatto and Uang, 2003; Pardoen et al., 2003). Numerous numerical models for wood shearwalls have been developed in the past two decades. One recent model that is widely recognized and accepted in both the wood engineering and research communities as an accurate hysteretic model for a wood shearwall is the CASHEW model (Folz and Filiatrault, 2001).

In seismic design of woodframe structures, engineered shearwalls (with hold-downs) are used to prevent uplift and to ensure a racking mode of deformation. This is consistent with the CASHEW modeling assumption that a shearwall acts as a mechanism that deforms into a parallelogram as the top of the wall is displaced. The model is able to predict load-displacement response at the top of the wall by keeping track of the load-slip response of the connectors as well as the relative movements of the shearwall components (sheathing panels and framing members). The in-plane bending of the framing members (or studs) has very little effect on the overall shearwall response (Gupta and Kuo, 1985). Based on this assumption, the framing members are modeled as rigid elements with pin-ended connections, and thus do not contribute to the lateral stiffness of shearwalls. The main source of lateral stiffness of wood shearwalls therefore comes from the inelastic load-slip response of the sheathing-to-framing connectors.

In the CASHEW model, the load-displacement behavior at the top of the wall is modeled using a nonlinear SDOF spring. A total of ten parameters are required to completely describe the hysteretic response of the nonlinear SDOF spring. However, only the backbone curve parameters are used in the proposed DDD procedure. Using only the backbone response of shearwalls allows the DDD procedure to be simplified as a design tool that can be used easily by engineers without having to build a complex nonlinear numerical model for the complete woodframe structure, and yet which provides a good estimate of story drifts. The envelope response of a wood shearwall is modeled by the following five-parameter nonlinear equation (Figure 4):

$$F_b(\delta) = \begin{cases} \left[ 1 - e^{-\frac{K_0}{F_0}\delta} \right] (r_1 K_0 \delta + F_0) & \text{for } \delta \leq \delta_u \\ F_u + r_2 K_0 (\delta - \delta_u) & \text{for } \delta > \delta_u \end{cases} \quad (14)$$

The exponential function used to describe the ascending branch of the envelope curve was first proposed by Foschi (1974) and has been used to model the ascending backbone envelope for the CASHEW model. Parameter  $K_0$  is the initial tangent stiffness of the backbone curve. As shown in Figure 4, as the displacement at the top of the wall,  $\delta$ , increases, the restoring force,  $F_b$ , asymptotically approaches the line given by  $r_1 K_0 \delta + F_0$  and the tangent stiffness degrades towards  $r_1 K_0$ . The restoring force continues to increase

until it reaches its maximum load-carrying capacity,  $F_u$ . The maximum force,  $F_u$ , and the associated displacement,  $\delta_u$ , are defined implicitly at the intersection point of the two functions. The post-peak envelope behavior is described by a linear line with a negative slope,  $r_2K_0$ .

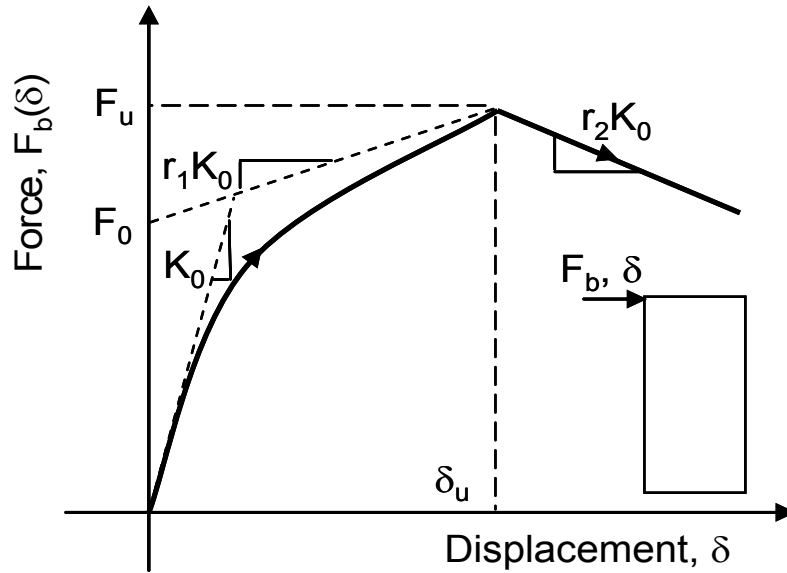


**Figure 4:** Shearwall backbone curve parameters.

### 3.4 Equivalent Linearization of Nonlinear Backbone Curve

The displacement-based design procedure originally proposed by Priestley (1998), and later adapted by Filiatrault and Folz (2002) for woodframe buildings, characterizes the actual nonlinear structure by the secant stiffness,  $k_s$ , at a target displacement,  $\delta_t$ , and an equivalent viscous damping representative of the global damping behavior of the whole structure. The complexity of this procedure lies in the determination of the equivalent viscous damping ratio and the need to perform more advanced pushover analyses of the complete structures, often comprising a large number of complex and interconnected assemblies. The proposed multi-story DDD procedure eliminates the needs for both conducting pushover analysis and determining an equivalent viscous damping ratio by performing linearization at the assembly level (shearwall). A substitute linear system is determined such that the linear elastic model with an equivalent stiffness,  $k_{eq}$ , can be used to approximate the work done or the energy stored in an actual nonlinear wood shearwall at a target displacement (Figure 5).

The energy stored in shearwalls,  $E_{NL}$ , at a target displacement,  $\delta_t$ , is equal to the area under the nonlinear backbone curve.

$$E_{NL} = \int_0^{\delta_t} F_b(\delta) d\delta \quad (15)$$

The strain energy,  $E_L$ , stored in an equivalent linear system is given by:

$$E_L = \frac{1}{2} k_{eq} \delta_t^2 \quad (16)$$

Equating the energy stored in the nonlinear system and the strain energy of the linear system and solving for the equivalent stiffness yields,

$$k_{eq} = \frac{2E_{NL}}{\delta_t^2} \quad (17)$$

Note that Eqn (17) cannot be evaluated at  $\delta_t = 0$  directly. However,  $k_{eq}$  approaches the initial stiffness,  $K_0$ , as  $\delta_t \rightarrow 0$ . At a non-zero target displacement,  $k_{eq}$  is always smaller than  $K_0$  and larger than the secant stiffness  $k_s$  (Figure 5). This linearization approach eliminates the need for estimating an equivalent viscous damping since the energies stored in both systems at  $\delta_t$  are equal and  $k_{eq}$  is an approximation of the ‘average stiffness’ of the actual nonlinear backbone curve at  $\delta_t$ .

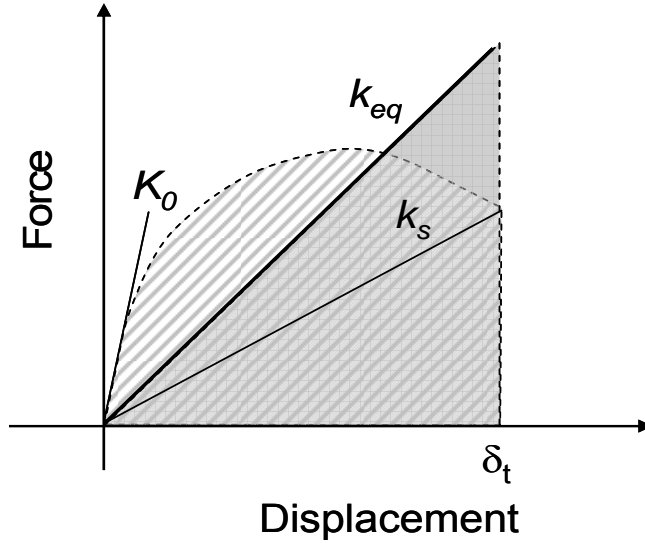


**Figure 5:** Equivalent linearization of nonlinear backbone curve.

### 3.5 Shearwall Backbone Design Table

In North American light-frame construction, wood shearwalls are typically sheathed by 1.22 m x 2.44 m (4 ft x 8 ft) (plywood or oriented strand board, OSB) panels oriented vertically or horizontally on the exterior. Gypsum wallboard (GWB) panels, generally, oriented horizontally, are used on the interior. The sheathing panels are often cut into narrower strips when necessary to fit around the windows or door openings. Studs are commonly spaced at either 400 mm or 600 mm (16 in or 24 in) on center. Typical spacings for the sheathing-to-framing connectors are 50, 75, 100 and 150 mm (2, 3, 4 and 6 in) on the perimeter and 300 mm (12 in) in the interior of the sheathing panel.

To assist with the shearwall selection process in the proposed DDD procedure, design tables that contain the shearwalls backbone parameters were developed for walls built with different types of connectors, nailing patterns and panel widths. The CASHEW program, along with available shearwall test data, was used to generate the design tables. Table 6 shows one example of a design table for 2.44 m (8 ft) high walls with 11 mm thick (7/16 in) OSB connected to nominal 50 mm x 100 mm (2 in x 4 in) Hem-Fir studs spaced at 400 mm (16 in) on-center using 8d common nails (63.5 mm (2.5 in) long x 3.3 mm (0.131 in) in diameter). The hysteretic parameters for the 8d common nails were extracted from results of the actual cyclic nail tests (Ekiert and Hong, 2006) conducted at the University at Buffalo as part of the NEESWood benchmark shake table test program (Filiatrault et al., 2007).

The proposed DDD procedure adopts the traditional segmented shearwall design approach, where only the full-height segments in a shearwall are considered and the sheathing panels above and below the openings are ignored. Under pure racking deformation (without uplift), uniform in-plane shear deformation is developed and all the full-height segments in a shearwall undergo the same lateral displacement. Figure 6 shows an example shearwall with a pedestrian door opening. The backbone response of this shearwall can be approximated by adding up the backbone curves of the four full-height segments indicated in the figure. This summing rule allows for a quick estimate of the backbone response of virtually any shearwall using only the three panel widths, 0.76 m, 0.91 m and 1.22 m (2.5 ft, 3 ft and 4 ft), shown in Table 6. Also shown in Table 6 are the equivalent stiffness values at various target drift levels calculated using Eqn (17). These pre-calculated equivalent stiffness values allow designers to perform shearwall selection based on the required story stiffness determined from a modal analysis. The procedure used to determine the required story stiffness is discussed next.

**Table 6:** Displacement-based shearwall design table for walls built with studs spaced at 400 mm (16 in) on-center and OSB attached using 8d common nails.

Sheathing	Panel Width (m)	Nail Spacing (mm) ext./int.	Panel ID	Backbone Parameters						Equivalent Stiffness, $k_{eq}$ (kN/mm) at Target Drift					
				$K_0$ (kN/mm)	$r_1$	$r_2$	$\delta_u$ (mm)	$F_0$ (kN)	$F_u$ (kN)	Drift (% of Wall Height)					
OSB*	0.76	50/300	c1	1.34	0.040	-0.083	104	18.9	24.5	1.05	0.85	0.71	0.60	0.53	0.47
		75/300	c2	1.12	0.038	-0.070	100	13.0	17.3	0.83	0.65	0.53	0.45	0.39	0.34
		100/300	c3	0.95	0.037	-0.062	97	9.9	13.3	0.69	0.53	0.42	0.35	0.30	0.27
		150/300	c4	0.73	0.035	-0.055	94	6.7	9.1	0.51	0.38	0.30	0.25	0.21	0.19
	0.91	50/300	c5	1.73	0.042	-0.096	91	24.6	31.2	1.36	1.10	0.92	0.79	0.69	0.61
		75/300	c6	1.43	0.042	-0.075	85	16.1	21.2	1.06	0.83	0.67	0.57	0.49	0.43
		100/300	c7	1.21	0.041	-0.066	83	12.1	16.2	0.87	0.66	0.53	0.44	0.38	0.33
		150/300	c8	0.94	0.039	-0.055	80	8.2	11.1	0.64	0.48	0.38	0.31	0.27	0.23
	1.22	50/300	c9	2.51	0.037	-0.126	74	37.1	43.7	1.98	1.61	1.35	1.16	1.01	0.90
		75/300	c10	2.18	0.042	-0.099	70	24.8	31.2	1.62	1.26	1.03	0.87	0.75	0.66
		100/300	c11	1.91	0.043	-0.083	67	18.7	24.1	1.36	1.03	0.83	0.69	0.59	0.52
		150/300	c12	1.55	0.042	-0.070	64	12.9	17.1	1.04	0.77	0.61	0.50	0.43	0.37
OSB* & GWB**	0.76	50/300	c25	1.50	0.025	-0.075	104	20.7	24.5	1.16	0.93	0.76	0.65	0.56	0.49
		75/300	c26	1.29	0.021	-0.061	98	14.8	17.4	0.94	0.73	0.59	0.49	0.42	0.37
		100/300	c27	1.13	0.017	-0.053	95	11.7	13.4	0.80	0.60	0.48	0.40	0.34	0.29
		150/300	c28	0.92	0.011	-0.047	91	8.5	9.4	0.63	0.46	0.36	0.29	0.25	0.21
	0.91	50/300	c29	2.00	0.026	-0.084	91	27.0	31.6	1.53	1.22	1.01	0.85	0.74	0.65
		75/300	c30	1.73	0.022	-0.064	85	18.6	21.8	1.24	0.95	0.76	0.63	0.54	0.47
		100/300	c31	1.52	0.018	-0.054	81	14.6	16.8	1.05	0.78	0.62	0.51	0.43	0.37
		150/300	c32	1.26	0.012	-0.044	77	10.7	11.8	0.83	0.60	0.46	0.38	0.32	0.27
	1.22	50/300	c33	2.92	0.023	-0.110	75	39.3	44.2	2.24	1.78	1.46	1.24	1.07	0.94
		75/300	c34	2.64	0.021	-0.084	70	27.9	31.7	1.89	1.44	1.14	0.95	0.81	0.70
		100/300	c35	2.40	0.017	-0.069	67	22.0	24.8	1.63	1.21	0.94	0.77	0.65	0.56
		150/300	c36	2.07	0.012	-0.053	63	16.3	17.8	1.33	0.94	0.72	0.58	0.49	0.42

\*11mm OSB (shear modulus of panel = 1.241 kN/mm<sup>2</sup>) connected to nominal 50 mm x 100 mm Hem Fir studs at 400 mm o.c. using 8d common nail (63.5 mm long x 3.3 mm in diameter)

\*\*12.7mm drywall, 31.8 mm long #6 bugle head screws @ 400mm o.c. on vertical studs only

\*\* Shaded values are used in the design of an example three-story woodframe building.

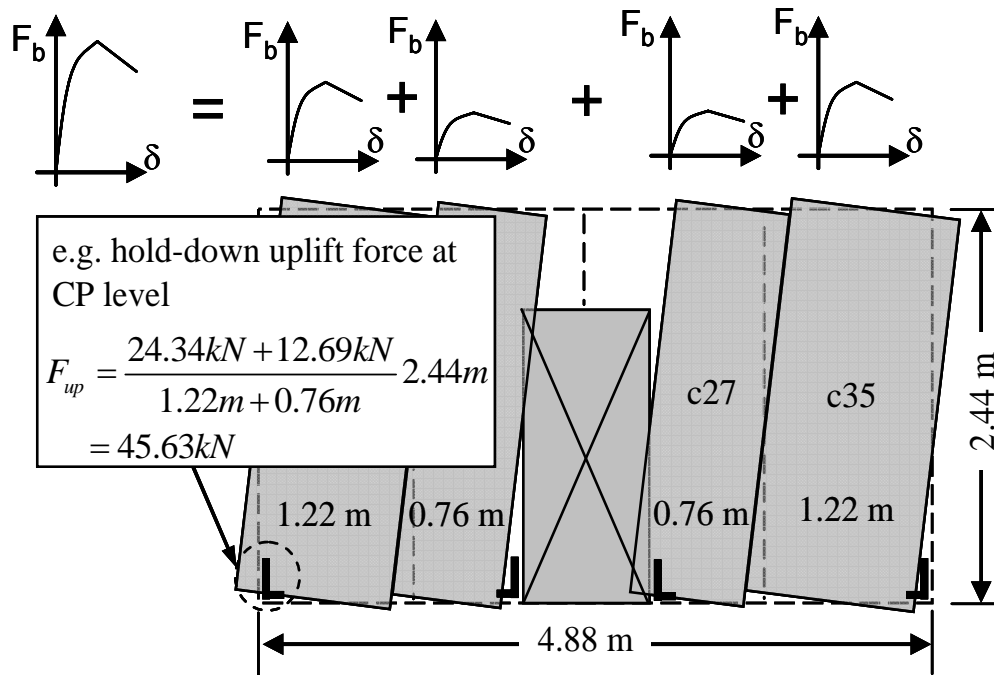


**Figure 6:** Summation of shearwall segment backbone curves.

### 3.6 Normalized Modal Analysis

The structural model that forms the basis for the proposed DDD procedure for multistory wood structures is derived from the widely used modal analysis approach. The model is based on equivalent linearization of a nonlinear multi-degree of freedom (MDOF) system in which the story stiffness of the linear elastic MDOF system is estimated with equivalent stiffness at the target inter-story drift.

Consider a multistory structure (as shown in Figure 7) with symmetric-plan about the two horizontal directions and having rigid floor diaphragms. The structure can be analyzed independently in the two lateral directions. The natural frequencies,  $\omega_n$ , and mode shapes,  $\phi_n$ , can be determined by solving the following eigenvalue problem:

$$[K - \omega_n^2 M] \phi_n = 0 \quad (18)$$

where  $K$  and  $M$  are the stiffness and mass matrices. The mass matrix is a diagonal matrix,

$$M = m \begin{bmatrix} 1 & 0 & 0 \\ 0 & \beta_{m2} & 0 \\ 0 & 0 & \beta_{m3} \end{bmatrix} \quad (19)$$

where  $m$  is the total lumped mass for first floor and  $\beta_{mj}$  is the  $j^{\text{th}}$  floor mass ratio (relative to the first floor). Accordingly, the stiffness matrix is given by,

$$K = k \begin{bmatrix} 1 + \beta_{k2} & -\beta_{k2} & 0 \\ -\beta_{k2} & \beta_{k2} + \beta_{k3} & -\beta_{k3} \\ 0 & -\beta_{k3} & \beta_{k3} \end{bmatrix} \quad (20)$$

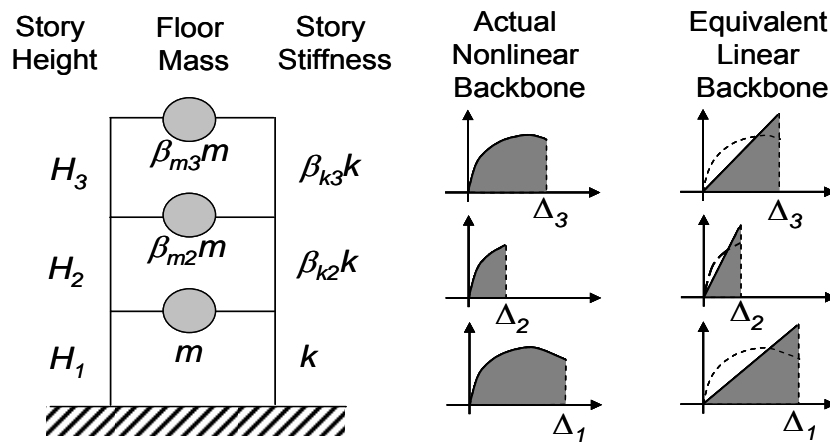


**Figure 7:** Equivalent linearization of a nonlinear MDOF system.

Where  $k$  is the first-floor stiffness and  $\beta_{kj}$  is the  $j^{\text{th}}$  floor stiffness ratio (relative to the first floor). At the beginning of a design procedure, floor masses are generally known or can be estimated. The lateral stiffness required for each floor, however, is unknown. Designers can specify or estimate the relative floor stiffness,  $\beta_{kj}$ . Thus, the first-floor stiffness,  $k$ , is the only design parameter to be determined.

The natural frequencies,  $\omega_n$  (rad/sec), and periods,  $T_n$  (sec), for the  $n$ -th mode are given by,

$$\omega_n = \alpha_n \sqrt{k/m} \quad (21)$$

$$T_n = \frac{2\pi}{\alpha_n \sqrt{k/m}} = \frac{\bar{T}}{\alpha_n} \quad (22)$$

where  $\bar{T}$  is defined as the normalized first-story period. The natural frequency parameters,  $\alpha_n$ , in Eqns (21) and (22) can be obtained by setting  $k$  and  $m$  equal to unity and solving Eqn (18). The natural vibration mode corresponding to each frequency is a vector given by  $\phi_n$ , where subscripts  $n$  and  $j$  are mode and floor numbers, respectively.

Commonly used numerical analysis software packages, such as MathCAD<sup>®</sup> and Matlab<sup>®</sup>, have built-in functions that can be used to solve the eigenvalue problem. In MathCAD<sup>®</sup>, functions *genvals(.)* and *genvecs(.)* provide the solutions for eigenvalues,  $\alpha_n^2$ , and eigenvectors,  $\phi_n$ :

$$\alpha_n = \sqrt{\text{genvals}(K, M)} \quad (23)$$

$$\phi_{jn} = \text{genvecs}(K, M) \quad (24)$$

Similarly, the Matlab<sup>®</sup> function *eig(.)* can be used to obtain both  $\alpha_n$  and  $\phi_{jn}$ :

$$[\phi_{jn}, \alpha_n^2] = \text{eig}(K, M) \quad (25)$$

The extent to which the  $n^{\text{th}}$  mode is excited by the ground motion is given by the modal participation factors,  $\Gamma_n$

$$\Gamma_n = \frac{\sum_{j=1}^{N_{\text{floor}}} \beta_{mj} \phi_{jn}}{\sum_{j=1}^{N_{\text{floor}}} \beta_{mj} (\phi_{jn})^2} \quad (26)$$

where  $N_{floor}$  is the total number of floors of the structure. Since limiting inter-story drift is the main objective for the DDD procedure, a more useful measurement of the contribution of each mode to the total inter-story drift is defined here as the inter-story drift factor,  $\gamma_{jn}$  :

$$\gamma_{jn} = \Gamma_n (\phi_{jn} - \phi_{j-1,n}) \quad (27)$$

Note that solutions for modal participation factors,  $\Gamma_n$ , are not unique and are dependent on how the modes,  $\phi_n$ , are normalized. On the other hand, inter-story drift factors,  $\gamma_{jn}$ , are independent of how the modes are normalized. Once  $\alpha_n$  and  $\gamma_{jn}$  are determined, they can be used to generate the design inter-story drift spectra by modifying the code specified acceleration design response spectrum.

### 3.7 Design Inter-story Drift Spectra

The design acceleration response spectrum can be converted into a displacement response spectrum,  $S_d$ , using the following:

$$S_d(T) = \left( \frac{T}{2\pi} \right)^2 S_a(T) \quad (28)$$

in which  $S_d$  represents the displacement response of the overall structure modeled as an elastic SDOF system. In performance-based seismic design, inter-story drift is used to quantify the damage state or performance of the structure. Therefore, the displacement-based procedure is formulated herein in terms of the inter-story drift response.

The natural frequency parameters,  $\alpha_n$ , and inter-story drift factors,  $\gamma_{jn}$ , are used to create the inter-story drift spectra. Figure 8 illustrates the process of constructing an inter-story drift spectrum for the  $j^{\text{th}}$  floor normalized to the first-story period,  $\bar{T}$ . The first step in generating an inter-story drift spectrum is to perform a modal expansion of the displacement response spectrum for the overall structure modeled as an SDOF system, Eqn (28). The SDOF displacement response spectrum is expanded into its inter-story drift modal components for the floor considered. The contribution of each mode to the total inter-story drift is determined by multiplying the period,  $T$ , (x-axis) by  $\alpha_n$ , and multiplying the spectral displacement,  $S_d$ , (y-axis) by ratio of  $\gamma_{jn} / H_j$ , where  $H_j$  is the inter-story height of the story considered. The square-root-of-sum-of-squares (SRSS) modal combination rule is then used to obtain the total inter-story drift,  $\Delta_j$  (% of story height), for each value of  $\bar{T}$ .

$$\Delta_j(\bar{T}) = \frac{1}{H_j} \sqrt{\sum_n \left[ \gamma_{jn} \left( \frac{\bar{T}}{\alpha_n 2\pi} \right)^2 S_a(\bar{T}/\alpha_n) \right]^2} \quad (29)$$

In general, the SRSS combination rule provides excellent peak response estimates for symmetric buildings with well-separated frequencies (Chopra, 2001). The modal expansion and combination procedures are incorporated into a single equation (29) which can be used to generate the inter-story drift spectra.

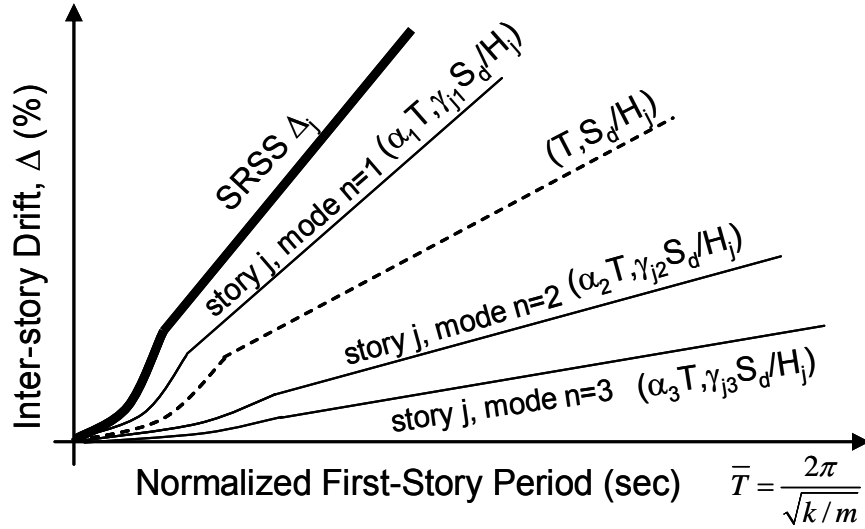


**Figure 8:** Construction of an inter-story drift spectrum.

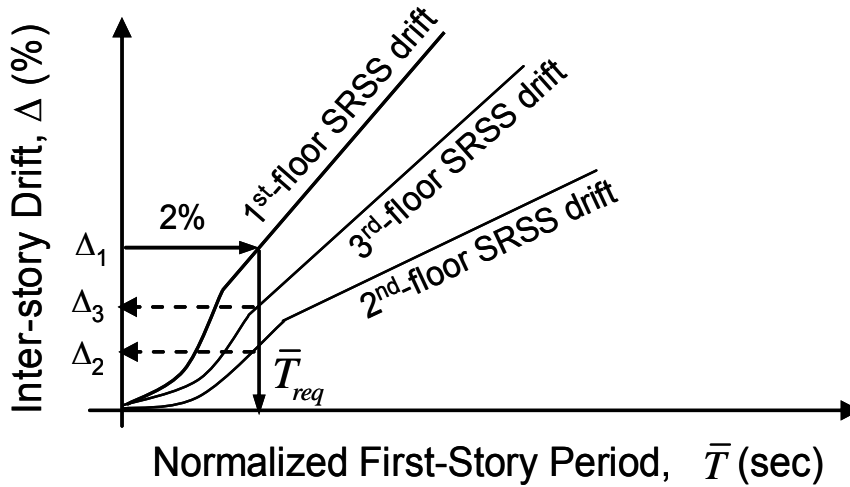


**Figure 9:** Determination of the required first-floor period.

### 3.8 Required Equivalent First-floor Period and Stiffness

The governing (i.e., weakest) floor in a building can be determined, graphically, by showing the inter-story drift spectra for each floor together on one figure. Consider, as an example, the inter-story drift spectra for a three-story building shown in Figure 9. The steepest drift response curve corresponds to the floor that will reach the design limit first. For the LS performance level, the drift limit is taken as 2%. A required normalized first-floor period,  $\bar{T}_{req}$ , can be obtained by locating the point on the inter-story drift spectrum for the governing floor that corresponds to 2% drift.

Knowing the required equivalent first-floor period, the story drifts for the remaining floors ( $\Delta_2$  and  $\Delta_3$ ) at the design limit can be obtained directly from Figure 9. Alternatively, the drift at each floor at the design limit can be computed using Eqn (29) at  $\bar{T} = \bar{T}_{req}$ . The required equivalent stiffness for each floor,  $(k_{eq})_j$ , can be calculated using the following equation once the required equivalent period is determined:

$$(k_{eq})_j = \left( \frac{2\pi}{\bar{T}_{req}} \right)^2 m \beta_{kj} \quad (30)$$

where  $m$  and  $\beta_{kj}$  are previously defined as the first-floor mass and stiffness ratios (relative to the first floor).

Once the required stiffness for each floor is determined, shearwall backbone database tables (e.g., Table 6) can be used to select wall segments that will provide the required story stiffness. For symmetric multi-story structures with rigid diaphragms (i.e., no torsion), all shearwall segments at the same level undergo the same lateral displacement. Therefore, direct summation of equivalent stiffnesses of all wall segments (obtained from Table 6) at a target drift level provides the design equivalent story stiffness for the performance level being considered.

To design for multiple performance levels, the design process is repeated for each additional performance level starting with the construction of a new set of inter-story drift spectra for the target hazard level. The required story stiffness for each additional performance level is checked against the sum of the equivalent stiffnesses of all wall segments at the target drift profile. A final design is reached when a lateral load resisting system (combination of shearwall segments selected from the design tables) meets the drift limits for all performance levels.

### 3.9 Required Base Shear, Story Shear and Uplift Force

Once the design process is completed for all performance levels and a set of shearwall segments is selected, the story shear force,  $V_j$ , and base shear (first-story shear force) can be determined by summing the actual shearwall backbone forces ( $F_b$  given by Eqn (14)) at the target drift profile :

$$V_j = \sum_{walls} \begin{cases} F_b \left( \Delta_j \left( \bar{T}_{req} \right) h \right) & \text{for } \Delta_j \left( \bar{T}_{req} \right) h < \delta_u \\ F_u & \text{for } \Delta_j \left( \bar{T}_{req} \right) h \geq \delta_u \end{cases} \quad (31)$$

where  $h$  is the height of the shearwalls. The story shear force at the  $j^{\text{th}}$  floor can be found by summing the shearwall forces at that story. Conservatively, the story shear force can be estimated as the sum of the peak backbone forces,  $F_u$ , listed in the shearwall design tables (e.g., Table 6). The story shear forces calculated using Eqn (31) can be used to size the anchor bolts at the foundation or design the connection elements between stories.

The backbone curve parameters listed in the design tables were developed for engineered shearwalls with hold-downs installed to prevent uplift. Hold-downs for overturning restraint are assumed to be placed at each end of the full-height shearwalls. The maximum uplift force,  $F_{up}$ , developed at the end studs can be estimated based on the height-to-width ratio of the full-height wall segment:

$$F_{up} = \frac{h}{\sum_{walls} B} \sum_{walls} \begin{cases} F_b \left( \Delta_j \left( \bar{T}_{req} \right) h \right) & \text{for } \Delta_j \left( \bar{T}_{req} \right) h < \delta_u \\ F_u & \text{for } \Delta_j \left( \bar{T}_{req} \right) h \geq \delta_u \end{cases} \quad (32)$$

where  $B$  is the width of individual shearwall panel. Design or selection of hold-down devices can be based on the maximum uplift force calculated using Eqn (32).

## 4. Design Example

### 4.1 Description of Three-Story Woodframe Structure

A three-story woodframe structure having plan dimensions of 4.88 m x 6.10 m (16 ft x 20 ft) and elevation views shown in Figure 10 was selected as an illustrative design example. The building layout is similar to the two-story benchmark structure tested under Task 1.1.1 of the CUREE-Caltech Woodframe project (Fischer et. al., 2001). The first floor layout of this example building is identical to the first floor of the two-story CUREE test structure and, the second and third floors are duplicates of the second floor of the CUREE test structure. The height of the structure from the base to the eaves of the roof is 8.23 m (27 ft), with a story height of 2.74 m (9 ft).

For this example, the design is limited to those shearwall configurations listed in Table 6. The shearwalls are sheathed on the exterior with 11 mm (7/16 in) OSB connected to the framing members using 8d common nails (63.5 mm (2.5 in) long x 3.3 mm (0.131 in) in diameter). Gypsum wallboard, 12.7 mm (1/2 in) thick, is used on the interior of the shearwalls. The shearwalls are framed using nominal 50 mm x 100 mm (2 in x 4 in) studs spaced at 400 mm (16 in) on-center. Effective seismic weights of 62 kN (13.9 kip) are assigned to the first and second floors, and 48 kN (10.8 kip) is used for the third floor. These seismic weights are based on the weights determined for the second

floor and roof diaphragms of the two-story CUREE benchmark structure (Folz and Filiatrault, 2001). The building is designed for the site described previously (Lat. 34.05° and Long. -118.242°) located in Los Angeles, California, assuming Site Class D (FEMA 356 soil classification).

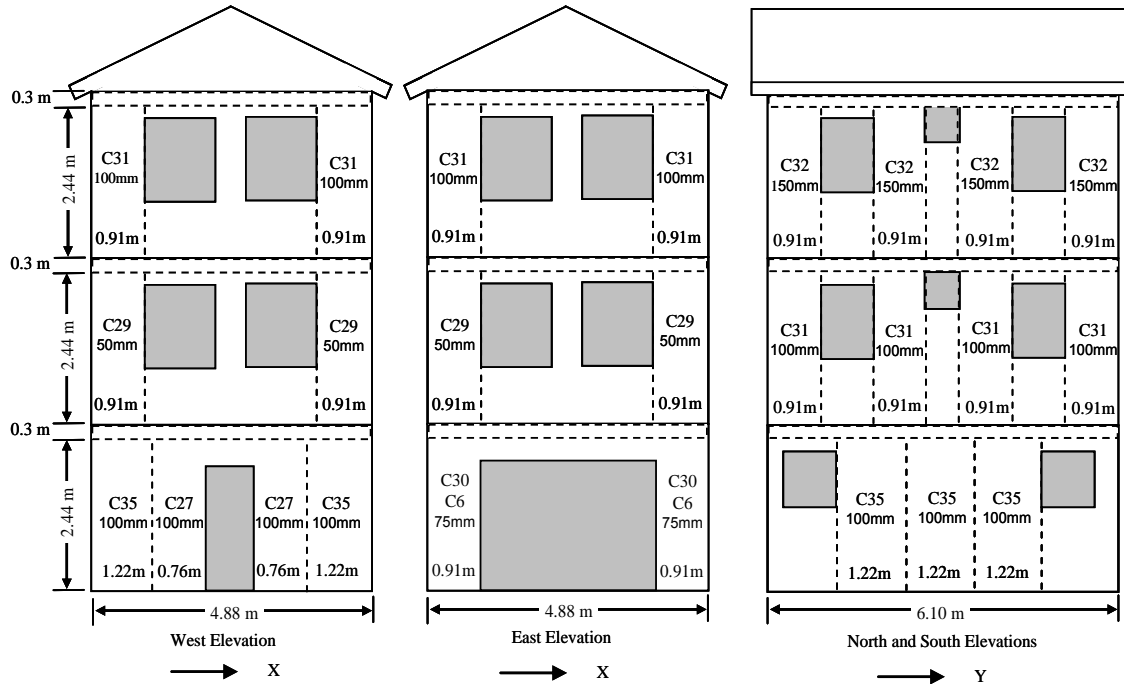


Figure 10: Elevation views of three-story woodframe structure.

## 4.2 Design Process

The example three-story building has a relatively symmetric plan with the exception of the east and west walls on the first floor. The building can be analyzed independently in the two lateral directions since torsional effects are assumed to be negligible for this geometrically symmetric building. The specific design steps, considering the X-direction (east and west walls) as an example are shown in Figure 2 and are described below.

### Step 1. Define Target Performance Levels

The three FEMA 356 performance levels (IO, LS, and CP) discussed previously are used as design objectives for the structure. The target hazard levels and drift limits are listed in Table 1. The corresponding design acceleration response spectra (based on the USGS 2002 hazard data and FEMA 356 procedure) are shown in Figure 3.

### Step 2. Determine the Mass and Stiffness Ratios

Obtaining the mass ratios,  $\beta_m$ , is straightforward. Knowing the effective seismic weights acting at each floor, the mass ratios (relative to the first floor) are 1.0, 1.0, and 0.77 for the first, second, and third floors, respectively. The target stiffness ratios,  $\beta_k$ , on the other hand, must be estimated based on some engineering judgment or experience. One way to establish initial estimates for  $\beta_k$  is to calculate the total available shearwall length, in the direction considered, for each story. The combined shearwall length for the first floor east and west walls is 5.78 m. The second and third floors both have 3.64 m available for full-height shearwalls (see Figure 10). Based on the available shearwall length, an initial estimate for  $\beta_k$  of 0.63 is assumed for the second and third floors.

### Step 3. Normalized Modal Analysis

Once the mass and stiffness ratios are determined, the normalized mass and stiffness matrices are easily formed using Eqns (19) and (20). Next, the frequency parameters  $\alpha_n$  and mode shapes,  $\phi_n$ , can be solved using any commercially available numerical packages (e.g., see Eqns 23-25). Knowing mode shapes  $\phi_n$ , the inter-story drift factors,  $\gamma_{jn}$ , can be computed directly using Eqn (27). The results for the normalized modal analysis for the X-direction are shown in Figure 11.

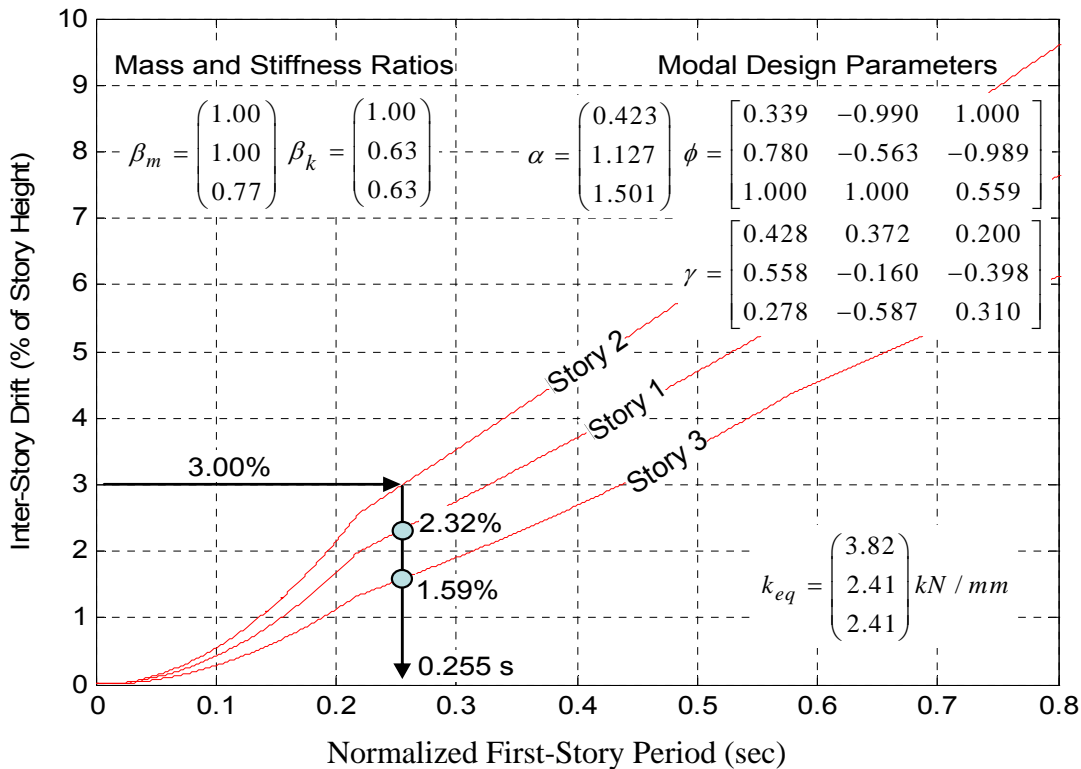


**Figure 11:** Direct displacement design for the CP performance level.

#### Step 4. Construct Inter-story Drift Spectra

The DDD procedure begins by considering the performance level associated with the most severe seismic demand (i.e., 2%/50yr event for the CP performance level). The inter-story drift spectra for the 2%/50yr hazard level are shown in Figure 11. These inter-story drift spectra are generated by modifying the code specified acceleration response spectrum (Figure 3) using Eqn. (29). Figure 11 shows that the second floor governs in the case of the CP performance level. The maximum normalized first-story period,  $\bar{T}_{req}$ , required to meet the 3% drift limit on the second floor is 0.255 seconds. At the CP design limit, one can expect the drifts at the first and third floors of 2.32% and 1.59%, respectively. Knowing the required first-floor period  $\bar{T}_{req}$ , the required equivalent stiffness at each floor is then determined using Eqn. (30). It is worth noting here that a design optimization can be performed at this step if desired. For example, one can increase the target stiffness ratio of the second floor and reduce the target stiffness of the third floor in attempt to obtain a uniform drift distribution across the stories.

#### Step 5. Select Shearwall Segments

After a target drift profile and associated required story stiffnesses are determined, Table 6 can be used to select shearwall segments. From step 4, the story stiffness required for the first floor is 3.82 kN/mm. In order to minimize torsional effects, each wall line (east and west walls) should have approximately the same stiffness (i.e., 1.91 kN/mm). The design for first-floor shearwalls begins with choosing panels to meet the east wall (garage wall) requirement. The garage wall must be built with two 0.91 m wide panels. Thus, possible options from Table 6 are panels c5 - c8 and panels c29 - c32. Based on the results of the normalized modal analysis (Figure 11), at the CP level, the first-floor drift (rounded to the nearest 0.5%) is about 2.5% drift (actual value is 2.32%). From Table 6, if only those panels with OSB+GWB are considered, using the panel with even the densest nailing schedule (c29) will not meet the stiffness requirement ( $2 \times 0.74 = 1.48$  kN/mm < 1.91 kN/mm). A possible solution is to use OSB on both the exterior and interior of the garage wall. One design that will meet this requirement is to combine panels c6 and c30 to provide an equivalent stiffness of 2.06 kN/mm at 2.5% drift (Table 7). For the first floor west wall (wall with pedestrian door), 1.22 m wide panels c35 and 0.71 m wide panels c27 are used to achieve an equivalent stiffness of 1.98 kN/mm (Table 7). The nail spacing selected for the first floor west wall is 100mm/300mm. The same shearwall selection criteria can be applied to the second and third floors. The final design for both the east and west walls is shown in Figure 10 and the design process for the CP performance level is summarized in Table 7.

#### Step 6. Verify Design Using the Actual Stiffness Ratios

The stiffness ratios determined from Step 2 (shown as initial  $\beta_k$  values in Table 7) were initial estimates or target values. The actual equivalent stiffness provided by the shearwalls at each floor varies slightly from the required equivalent stiffness. At the CP level, the actual stiffness ratios at the second floor increased slightly (from 0.63 to 0.64) while the third-floor stiffness ratio decreased slightly (from 0.63 to 0.61). As a final step, another normalized modal analysis is performed (using the actual values of  $\beta_k$ ) to determine new story drift estimates and required equivalent stiffnesses. Table 7 shows that the new drift predictions are below the CP drift limit (i.e., 3%) and the required

equivalent stiffnesses are lower than the actual equivalent stiffnesses provided. Thus, the design meets the CP performance requirements. The stiffness of the actual lateral force resisting system, parallel to the east and west walls, is about 9~10% higher than the minimum required stiffness (see last column of Table 7). This verification process completes the DDD procedure for one performance level.

**Table 7:** Displacement-based design of east and west walls for multiple performance levels.

		Initial Estimate			Shearwall Selection						Design Verification			
CP Level	Story	Initial $\beta_k$	Drift (%)	Required $k_{eq}$ (kN/mm)	Rounded Drift (%)	Actual $k_{eq}$ (kN/mm)					Actual $\beta_k$	Drift (%)	Required $k_{eq}$ (kN/mm)	$k_{eq}$ Actual / Required
						East	Panel ID	West	Panel ID	Total				
CP Level	1	1.00	2.32	3.82	2.50	2.06	2 c30 + 2 c6	1.98	2 c35 + 2 c27	4.04	1.00	2.36	3.71	1.09
	2	0.63	3.00	2.41	3.00	1.30	2 c29	1.30	2 c29	2.60	0.64	3.00	2.38	1.09
	3	0.63	1.59	2.41	1.50	1.24	2 c31	1.24	2 c31	2.48	0.61	1.67	2.26	1.10
LS Level	1	1.00	1.57	3.62	1.50	2.86	2 c30 + 2 c6	2.84	2 c35 + 2 c27	5.70	1.00	1.46	3.92	1.45
	2	0.64	2.00	2.32	2.00	1.70	2 c29	1.70	2 c29	3.40	0.60	2.00	2.35	1.45
	3	0.61	1.11	2.21	1.00	1.56	2 c31	1.56	2 c31	3.12	0.55	1.17	2.16	1.44
IO Level	1	1.00	0.73	5.14	1.00	3.56	2 c30 + 2 c6	3.62	2 c35 + 2 c27	7.18	1.00	0.84	4.28	1.68
	2	0.60	1.00	3.08	1.00	2.44	2 c29	2.44	2 c29	4.88	0.68	1.00	2.91	1.68
	3	0.55	0.58	2.83	0.50	2.10	2 c31	2.10	2 c31	4.20	0.58	0.62	2.48	1.69

### Step 7. Design for Additional Performance Levels

The east and west shearwalls were selected in step 5 considering the CP performance level. The shearwall combinations can then be checked at the LS and IO performance levels by repeating Steps 2 - 6. At Step 2, the actual  $\beta_k$  values for the CP level are used as the initial estimates of  $\beta_k$  for the analysis considering the LS performance level. Based on the results of the LS level modal analysis, the new drift predictions were about 1.5%, 2.0% and 1.0% for first, second, and third floors (rounded drift values in Table 7), respectively. At this stage, no selection of shearwalls is required. A new set of equivalent stiffnesses were determined from Table 6 using the drift values (rounded to the nearest 0.5%) at the LS level. The results show that the designed structure is about 45% stiffer than the minimum requirement at the LS level (last column in Table 7). Step 7 is repeated for the IO performance level and the results show that the stiffness of the structure is about 68% higher than the required stiffness at the IO performance level.

### Step 8. Computation of Story Shears and Uplift Forces

Using Eqn (31), the X-direction story shears for all three target performance levels are computed and are shown in Table 8. The peak backbone forces of shearwalls and the required story shears for the CP performance level are shown in Table 9. The base shear required in the X-direction to meet the CP performance is 154 kN. This base shear value can be used to size the anchor bolts for the foundation, for example. Table 8 also shows that in order to meet the CP requirement the connections between the first and the second floors must be able to carry 122 kN of story shear. Similarly, the connections for the

interface between the second and the third floors must be able to transfer 62 kN of story shear (at the CP performance level).

The maximum uplift forces of the full-height shearwall segments are computed using Eqn (32). Consider as an example, for the first floor west wall (wall with pedestrian door) in which 1.22 m wide panel c35 and 0.71 m wide panel c27 are used (Figure 6). The peak backbone forces for these two panels at the CP level are listed in Table 9. In order to meet the CP requirement, the hold-downs must be able to carry 45.63 kN (10.26 kip) of tensile force (see Figure 6).

Using the same design approach, the shearwalls in the Y-direction (north and south walls) were selected and are shown in Figure 10.

**Table 8:** X-direction design story shears for multiple performance levels.

Floor	Performance Level		
	CP	LS	IO
Story Shear (kN)			
1	154	143	124
2	122	115	94
3	62	58	48

**Table 9:** Determination of X-direction peak backbone forces and design story shears for the CP performance level.

Floor	Panel ID	Backbone Parameters						No. Panels	Design Drift (%)	Max. Displ. (mm)	Max. Backbone Force per Panel (kN)	Story Shear (kN)
		$K_0$ (kN/mm)	$r_1$	$r_2$	$\delta_u$ (mm)	$F_0$ (kN)	$F_u$ (kN)					
1	c6	1.43	0.042	-0.075	85	16.1	21.2	2	2.36	58	19.43	154
	c30	1.73	0.022	-0.064	85	18.6	21.8				20.65	
	c35	2.40	0.017	-0.069	67	22.0	24.8				24.34	
	c27	1.13	0.017	-0.053	95	11.7	13.4				12.69	
2	c29	2.00	0.026	-0.084	91	27.0	31.6	4	3.00	73	30.62	122
3	c31	1.52	0.018	-0.054	81	14.6	16.8	4	1.67	41	15.46	62

### 4.3 Verification of DDD using Nonlinear MDOF Dynamic Analyses

The three-story example structure designed according to the proposed displacement-based procedure was next analyzed using nonlinear time-history dynamic analyses. Three sets of bi-axial ground motions, representative of the seismic hazard associated with the IO, LS, and CP performance levels, were used. The selection of bi-axial historical earthquake records to characterize the design hazard levels followed the guidelines in Section 1.6.2.2 of FEMA 356 (2000). For each hazard level, an ensemble of 20 earthquakes was selected from the PEER Strong Motion Database (PEER, 2000) such that the SRSS (for the two horizontal components) of the 5%-damped acceleration spectrum for each earthquake matched the design acceleration response spectrum (shown in Figure 3) times 1.4 for periods below 1 sec. Figure 12 illustrates the 5%-damped acceleration response spectra for the individual record in an ensemble of ground motions for the LS hazard level, as well as the median response spectrum for the ensemble.

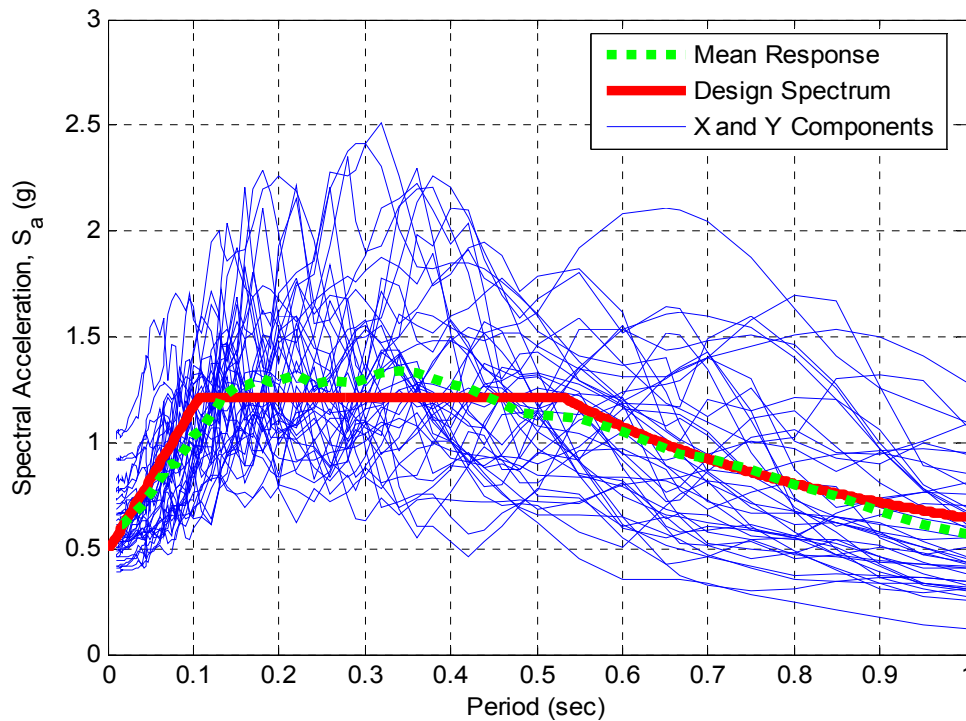


**Figure 12:** Response spectra for the 10%/50yr bi-axial ground motions.

The three-story building was modeled using a specialized nonlinear three-dimensional numerical analysis program, SAWS (Seismic Analysis of Wood Structures) program, developed for wood buildings (Folz and Filiatrault, 2001b). Rigid diaphragms with two translational and one rotational degrees of freedom were assumed for the roof and floor systems (Figure 13). Each shearwall segment was modeled as a nonlinear SDOF system using the hysteretic model in the CASHEW program. The load-

displacement response for each shearwall was predicted using CASHEW and a system identification procedure was used to obtain a set of ten parameters to describe the global hysteretic behavior of the shearwall. Note that the five backbone parameters used in the three-dimensional building model for the shearwall hysteretic elements were identical to those listed in Table 6. Since most of the damping is accounted for in the hysteresis model itself, only a very low amount of viscous damping (1% of critical damping) was assigned to the model for the purpose of maintaining numerical stability during the time-step integration.

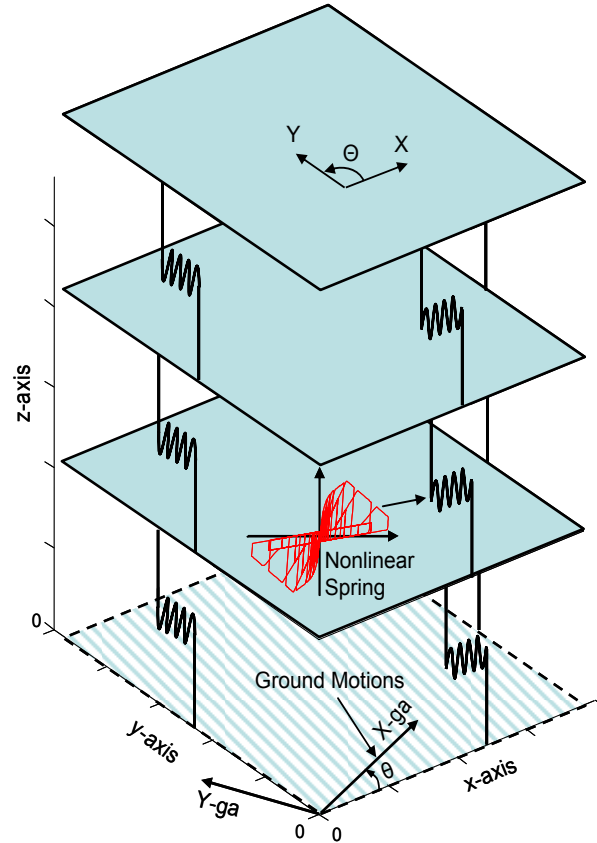


**Figure 13:** Three-dimensional nonlinear model for a three-story woodframe structure.

For each earthquake event, the two horizontal ground acceleration components were rotated from 0 to 90 degrees with respect to the axes of the building at 22.5 degree increment and a time-history analysis was performed for each orientation of the bi-axial ground motions. By rotating the set of ground motions, the worst-case scenario (in terms of the maximum drift) could be determined. Note that the maximum drifts for the two lateral directions might not occur at the same earthquake orientation.

The results of the nonlinear dynamic time history analyses for the CP performance level are presented in Figure 14. For the collapse prevention limit state, the three-story building designed according to the DDD approach meets the design objective since all mean inter-story drifts are below the 3% drift limit. According to FEMA 356

(2000), the average value can be used to determine the acceptability of a design when more than seven ground motions are used in the time-history analysis. Table 10 summarizes the mean peak drifts obtained from the time-history analyses for the three performance levels. The results show that the three-story building meets the IO, LS, and CP performance levels since the mean peak drifts are lower than the 1%, 2% and 3% drift limits, respectively. The controlling design is at the CP performance level since the critical wall has a mean peak drift (first floor Y-direction drift of 2.95%) closest to the design limit, i.e., 3%.

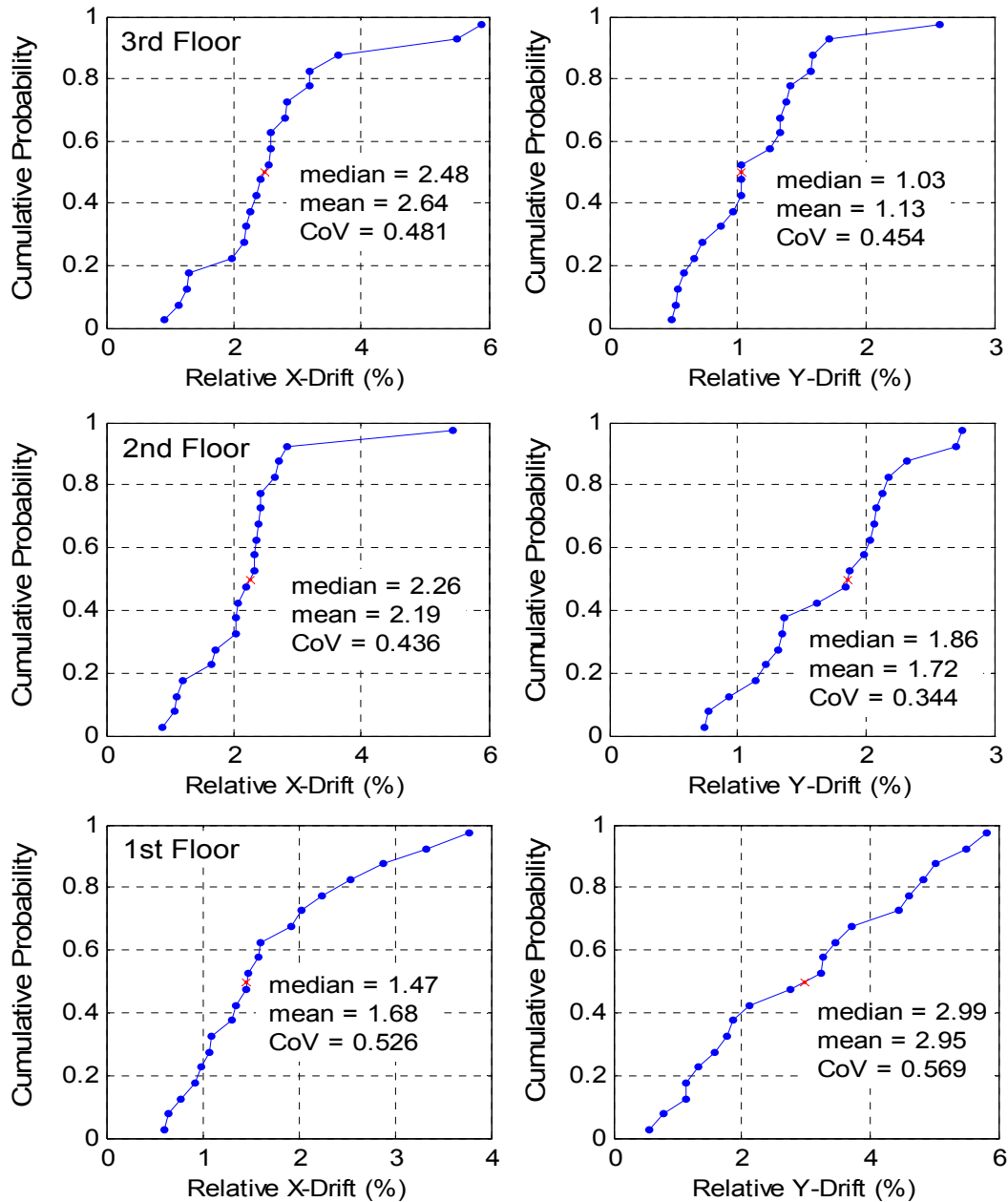


**Figure 14:** Peak drift distributions from nonlinear dynamic analyses (CP hazard level).

**Table 10:** Average peak drift responses from nonlinear dynamic analyses for different hazard levels.

Hazard Level	Mean Peak Drift (%) (CoV)					
	2%/50yr		10%/50yr		50%/50yr	
Floor	X	Y	X	Y	X	Y
1	1.68 (0.53)	2.95 (0.57)	0.92 (0.38)	1.27 (0.48)	0.48 (0.18)	0.56 (0.30)
2	2.19 (0.44)	1.72 (0.34)	1.39 (0.21)	0.92 (0.30)	0.68 (0.26)	0.49 (0.25)
3	2.64 (0.48)	1.13 (0.45)	1.30 (0.30)	0.68 (0.31)	0.69 (0.37)	0.39 (0.34)

\* Shaded values are controlling drifts for a given hazard level.

A more rigorous way of validating the proposed design procedure is to compare the expected drift level of the designed structure to the actual mean drift profile obtained from the dynamic time-history analyses. Recall that the ratios of design-to-required stiffness in the X-direction are about 1.09, 1.45 and 1.68 for the CP, LS and IO performance levels, respectively (see last column of Table 7). In other words, the designed structure is about 9%, 45% and 68% stiffer than the minimum requirements at the CP, LS and IO performance levels, respectively. Assume that the expected drift and the ratios of design-to-required stiffness are inversely proportional, the drift demand of the designed structure can be estimated at each performance level by taking the ratio of the drift limit to the stiffness ratio. Based on this assumption, the designed structure is expected to reach 2.75%, 1.38% and 0.60% drifts in the X-direction at the CP, LS and IO hazard levels, respectively. From the time-history analyses, average peak drifts of the controlling floors in the X-direction for the CP, LS and IO hazard levels are 2.64%, 1.39%, and 0.69%, respectively (Table 10). The close match between the design inter-story drifts and the mean peak drifts obtained from time-history analyses further serves to validate the proposed procedure.

## 5. Conclusions

A direct displacement-based seismic design procedure for multi-story woodframe buildings has been presented. Inter-story drift is assumed to be the relevant design parameter since drift has been found to be a key predictor of damage in wood structures. The proposed design procedure is applicable to woodframe structures of regular shape with relatively symmetric plan and rigid diaphragms (i.e., no torsional effects). The design process does not require the engineer to perform complex nonlinear dynamic time-history analysis of the complete structure. Instead, only simple modal analysis and information describing the backbone curves of the participating shearwalls are needed. Design tables that contain the backbone curve information for commonly used shearwall configurations were developed using a mechanistic shearwall model that has been verified through actual full-scale shearwall tests. To illustrate the application of the displacement-based seismic design procedure, the design of a three-story building was considered. The structure designed according to the proposed method was evaluated through nonlinear time-history analyses using earthquakes representative of the different

hazard levels considered. The results showed that the design inter-story drift profiles closely matched the average maximum inter-story drift profiles obtained from the nonlinear time-history analyses, thereby validating the proposed procedure.

Displacement-based design procedure has several advantages over current force-based procedures. The proposed displacement-based procedure is tailored specifically for performance-based engineering where multiple target objectives can be achieved simultaneously. Unlike the force-based procedures, the displacement-based approach does not require the determination of a yield displacement or an  $R$  factor. Furthermore, information about the inter-story drift distribution is also revealed during the displacement-based design process allowing the designer to optimize the structure for a target drift profile, if desired. The proposed direct displacement design procedure can be extended to include torsional effects arising from irregular plans and/or flexible diaphragms.

## References

- American Society of Civil Engineers (ASCE) (2005). *Minimum Design Loads for Buildings and Other Structures* (ASCE/SEI 7-05), American Society of Civil Engineers, Reston, VA.
- Camelo, V., Beck, J., and Hall, J. (2001). *Dynamic Characteristics of woodframe structures*, CUREE Report W-11, Task 1.3.3, Consortium of Universities for Research in Earthquake Engineering, Richmond, CA.
- Chopra, A. K. (2001). *Dynamics of Structures: Theory and Applications to Earthquake Engineering*, Second Edition, Prentice-Hall Inc., Upper Saddle River, NJ.
- Ekiert, C. and Hong, J. (2006). "Framing-to-Sheathing Connection Tests in Support of NEESWood Project," Network of Earthquake Engineering Simulation Host Institution: State University of New York at University at Buffalo, Buffalo, NY.
- FEMA (2000). *Prestandard and Commentary for the Seismic Rehabilitation of Buildings*, FEMA 356, Federal Emergency Management Agency, Washington, DC.
- Filiatrault, A., and Folz, B. (2002). "Performance-based seismic design of wood framed buildings," *ASCE Journal of Structural Engineering*, 128(1): 39-47.
- Filiatrault, A., Epperson, M., and Folz, B. (2004). "Equivalent Elastic Modeling for the Direct-Displacement-Based Seismic Design of Wood Structures," *ISET Journal of Earthquake Technology*, 41(1): 75-99.
- Filiatrault, A., Christovasilis, I., Wanitkorkul, A., and Folz, B. (2006). "Displacement-Based Seismic Design of Light-Frame Wood Buildings," *Proceedings of the 9<sup>th</sup> World Conference on Timber Engineering*, Portland, OR.
- Filiatrault, A., Wanitkorkul, A., Christovasilis, I.P., van de Lindt, J., Symans, M., Rosowsky, D., and Davidson, R. (2007). "Experimental Seismic Performance Evaluation of a Full-scale Woodframe Building," *Proceedings of the 2007 Structures Congress*, Long Beach, CA.
- Fischer, D., Filiatrault, A., Folz, B., Uang, C-M, and Seible, F. (2001). *Shake Table Tests of a Two-Story Woodframe House*, CUREE Report W-06, Task 1.1.1, Consortium of Universities for Research in Earthquake Engineering, Richmond, CA.
- Folz, B., and Filiatrault, A. (2001a). "Cyclic analysis of wood shear walls," *ASCE J. Struct. Eng.*, 127(4): 433-441.
- Folz, B., and Filiatrault, A. (2001b). *A Computer Program for Seismic Analysis of Woodframe Structures*, CUREE Report W-21, Task 1.5.1, Consortium of Universities for Research in Earthquake Engineering, Richmond, CA.

- Foschi, R.O. (1974). "Load-slip Characteristics of Nails," *Wood Science*, 7(1), 69-76.
- Gatto, K. and Uang, C. (2003). "Effects of Loading Protocol on the Cyclic Response of Woodframe Shearwall," *ASCE J. Struct. Eng.*, 129(10): 1384-1393.
- Gupta, A.K., and Kuo, G.P. (1985). "Behavior of Wood-framed Shear Walls." *ASCE J. Struct. Eng.*, 111(8): 1722-1733.
- Holmes, W.T. and Somers, P. (1996), *Northridge Earthquake of January 17, 1994 Reconnaissance Report – Volume 2*, Earthquake Engineering Research Institute (EERI), 1995-03/2, Supplement C to Volume 11, Oakland, CA.
- International Code Council (ICC) (2006). *International Building Code*, Building Officials and Code International Code Council Inc., Country Club Hills, IL.
- Krawinkler, H. (1999). "Challenges and Progress in Performance-based Earthquake Engineering." *International Seminar on Seismic Engineering for Tomorrow*, Tokyo, Japan.
- Pardoen, G., Waltman, A., Kazanjy, R., Freund, E. and Hamilton, C. (2003). *Testing and Analysis of One-Story and Two-Story Shearwalls under Cyclic Loading*, CUREE Report W-25, Task 1.4.4, Consortium of Universities for Research in Earthquake Engineering, Richmond, CA.
- Pacific Earthquake Engineering Research Center (PEER) (2000). "PEER Strong Motion Database," <<http://peer.berkeley.edu/smcat/>>, Jan. 10, 2006.
- Priestley, M.J.N., (1998). "Displacement-based approaches to rational limit states design of new structures," Keynote Address, *Proceedings of the 11<sup>th</sup> European Conference on Earthquake Engineering*, Paris, France.
- Structural Engineers Association of Southern California (SEAOSC) – University of California-Irvine (UCI). (2001). "Report of a Testing Program of Light-Framed Walls with Wood-Sheathed Shear Panels," *Final Report to the City of Los Angeles Department of Building and Safety*, December 2001.
- van de Lindt, J.W. (2005). "The Next Step for ASCE 16: Performance-Based Design for Woodframe Structures," *Proceedings of the 1<sup>st</sup> Invitational Workshop on Performance-Based Design of Woodframe Structures*, <<http://www.engr.colostate.edu/pbd/>>, May 10, 2007.
- van de Lindt, J.W., and Liu, H. (2006). "Correlation of Observed Damage and FEMA 356 Drift Limits: Results from One-Story Woodframe House Shake Table Tests," *Proceedings of the 2006 Structures Congress*, St. Louis, MO.